INVESTIGATIONS ON THE GEOMETRIC ACCURACY POTENTIAL OF ALOS/PRISM IMAGERY

S. Kocaman, A. Gruen
Institute of Geodesy and Photogrammetry, ETH-Hoenggerberg, CH-8093 Zurich, Switzerland
<skocaman><agruen>@geod.baug.ethz.ch

KEY WORDS: PRISM images, high resolution, pushbroom, sensor modelling, calibration, validation

ABSTRACT

High-resolution satellite images (HRSI) at sub-5m footprint are becoming increasingly available. A set of algorithms for processing of HRSI has been developed at the Institute of Geodesy and Photogrammetry (IGP), ETH Zurich and realized in a software suite called SAT-PP (Satellite Image Precision Processing). The SAT-PP features mainly include: GCP measurements, image georeferencing with RPC approach and various other sensor models, DSM generation with advanced multi-image geometrically constrained Least-Squares matching for Linear Array and single frame sensors, ortho-image generation, and feature extraction. The software has been used for processing of a number of high resolution satellite sensors, such as IKONOS, QuickBird, and SPOT-5 HRS/HRG.
The new generation Japanese remote sensing satellite ALOS (Advanced Land Observing Satellite) has three remote-sensing instruments onboard: PRISM (Panchromatic Remote-sensing Instrument for Stereo Mapping), AVNIR-2 (Advanced Visible and Near Infrared Radiometer type-2), and PALSAR (Cloud Phased Array type L-band Synthetic Aperture Radar).
PRISM is a panchromatic radiometer with 2.5-meter spatial resolution. It has three optical systems for forward, nadir and backward view. The photogrammetric processing of PRISM imagery has special requirements due to the Linear Array CCD sensor structure. The interior geometry and the exterior orientation have special characteristics, and the physical sensor model should be developed accordingly. As a Member of the ALOS Calibration/Validation Team, we have implemented new algorithms for the geometric processing of the PRISM images, in particular for the interior orientation and self-calibration. In addition, we have refined our physical sensor model according to the multiple optical camera heads of the sensor. Our rigorous model for the PRISM sensor is based on a modified bundle adjustment algorithm with the possibility to use two different trajectory models: the Direct Georeferencing Model and the Piecewise Polynomial Model. Both models were initially developed for modelling the trajectory of the airborne Linear Array CCD sensor imagery. Their implementations are modified according to the requirements of the PRISM sensor geometry. The self-calibration is introduced into the adjustment to model the systematic errors of the sensor and the system as a whole. The additional parameters for the self-calibration are defined in accordance with the physical structure of the PRISM cameras.
We have tested our methods of georeferencing and DSM generation using the PRISM datasets acquired over four different testfields (Piemont, Italy, Saitama, Japan, Thun/Bern, Switzerland, and Okazaki, Japan). The rigorous sensor model performs well and results in sub-pixel accuracy for georeferencing and point positioning in all testfields. The self-calibration model has been tested in two different phases of the project separately. In the initial phase, where no laboratory calibration data was available, the use of the self-calibration was essential to achieve good accuracy. However, in the latter phase the laboratory calibration data became available and the additional parameters became less significant. A detailed analysis of the DSM generation is presented in another publication.

1. INTRODUCTION

High-resolution satellite images (HRSI) have been widely used in recent years to acquire panchromatic and multispectral images in pushbroom mode for photogrammetric and remote sensing applications. Most of these sensors use Linear Array CCD technology for image sensing and are equipped with high quality orbital position and attitude determination devices like GPS, IMU systems and/or star-trackers. The recently launched high resolution satellite sensor ALOS/PRISM is also operating in the pushbroom mode, and has Linear Array CCD pixels with 2.5 meter ground resolution. It provides along-track quasi-simultaneous overlapping triplet imagery with three different viewing angles (forward, nadir and backward).

For the full exploitation of the potential of the Linear Array CCD sensors' data, the "classical" satellite image analysis methods must be extended in order to describe the imaging geometry correctly, which is characterized by nearly parallel projection in along-track direction and perspective projection in cross-track direction. In general the processing of this kind of images provides a challenge for algorithmic redesign and opens the possibility to reconsider and improve many photogrammetric processing components. In recent years, a large amount of research has been devoted to efficiently utilize these high spatial resolution imagery data. Examples for sensor modelling and image orientation can be found in (Baltsavias et al., 2001; Jacobsen, 2003; Grodecki and Dial, 2003; Fraser et al., 2002; Fraser and Hanley, 2003; Gruen and Zhang, 2003; Poli, 2005; Eisenbeiss et al., 2004).

We have developed a full suite of new algorithms and the software package SAT-PP (Satellite Image Precision Processing) for the precision processing of HRSI data. The software can accommodate images from IKONOS, QuickBird, SPOT5 HRG/HRS, Cartosat-1 and sensors of similar type to be expected in the future. The functionality to accommodate ALOS/PRISM imagery has been added in the context of the work of ALOS Calibration/Validation Team, organized by JAXA, Japan. Detailed information on the SAT-PP features can be found in Gruen et al. (2005).

For the georeferencing of aerial Linear Array sensor imagery, we have implemented a modified bundle adjustment algorithm with the possibility of using three different trajectory models (Gruen and Zhang, 2003). Two of those models, the Direct Georeferencing (DGR) Model and the Piecewise Polynomial Model (PPM) are modified for the special requirements of the PRISM sensor and extended with additional parameters (APs) for self-calibration, to possibly improve the camera's interior orientation parameters and to model other systematic errors.

The self-calibration model currently includes a total of 30 additional parameters for all 3 cameras.

The results of our work for georeferencing the early ALOS/PRISM imagery are presented in this paper. Although the images have particular radiometric problems (Gruen et al., 2007), the sensor orientation results are at a good level of accuracy. Our methods of data processing and the results of the empirical investigations in four different testfields are presented here.

2. ALOS/PRISM RIGOROUS SENSOR MODEL

The rigorous model for ALOS/PRISM sensor employs the collinearity equation and allows the use of the two trajectory models. The specifications of the PRISM interior and exterior geometries have been taken into account in the models. The PRISM sensor features one particular camera with a number of Linear Array CCD chips in the focal plane for each viewing angle. Three PRISM images per scene are acquired quasi-simultaneously in forward, nadir and backward viewing angles in along-track direction (Figure 1). Each scene has the stereoscopic viewing capability with the forward-nadir, the forward-backward and the nadir-backward images. The interval between the image acquisition time of the forward, nadir and backward images is 45 seconds each.

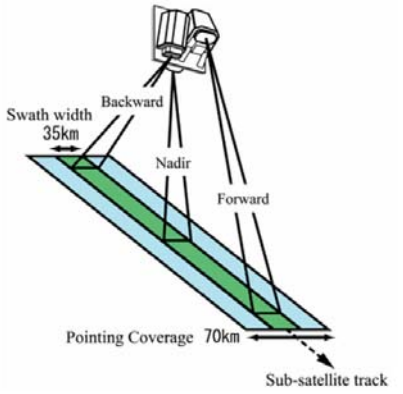

Figure 1. Observation geometry of triplet mode (Tadono et al., 2004).

The sensor platform trajectory values are provided in the image supplementary files. The attitude and position estimates are based on star tracker and GPS receiver data (Iwata, 2003). The given trajectory values are used as stochastic unknowns (observed values) in the adjustment.

Self-calibration is an efficient and powerful technique used for the calibration of photogrammetric imaging systems. If used in the context of a general bundle solution, it provides for object space coordinates or object features, camera exterior and interior orientation parameters, and models systematic errors as well (Gruen and Beyer, 2001). The self-calibration method is an alternative and supplementary method to the laboratory and testfield calibration. The method can use the laboratory calibration data as stochastic input in the adjustment.

Our work on the calibration of airborne Linear Array CCD sensors dates back to the year 2003 (Kocaman, 2003). The mathematical model and the practical test results from testfield datasets acquired with two different airborne Linear Array CCD sensors have been given by Kocaman et al. (2006). For the self-calibration of the PRISM imagery, we have initially defined 30 additional parameters in total for the 3 cameras. The parameters are described in accordance with the physical structure of the PRISM imaging sensors.

The Linear Array CCD structure of the nadir camera is demonstrated in Figure 2. The nadir camera contains 6 CCD chips , while the backward and the forward camera heads contain 8 CCD chips. When a swath width of 35 km is chosen, the PRISM images are generated using the data from up to 4 CCD chips in all viewing directions. The selection of the CCD chips to be used is project-dependent and done by the satellite operator.

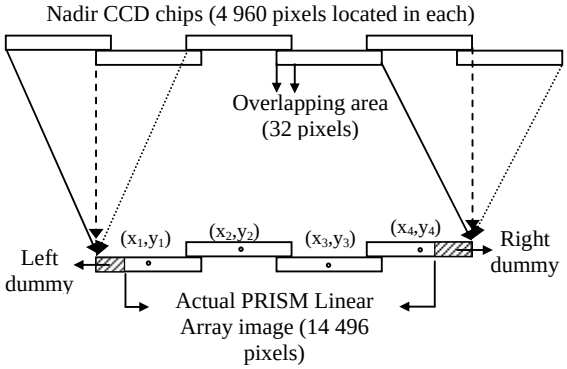

Figure 2. Linear Array CCD structure of the PRISM nadir viewing camera.

Each camera head has its own coordinate system definition. The *x*-axis is parallel to the flight direction, while the *y*-axis is parallel to the CCD line (across-track) direction (Figure 3). The origin of the image coordinate system is located in the principal point of the optical system. The CCD chip structures of the backward and forward looking cameras are similar and demonstrated also in Figure 3.

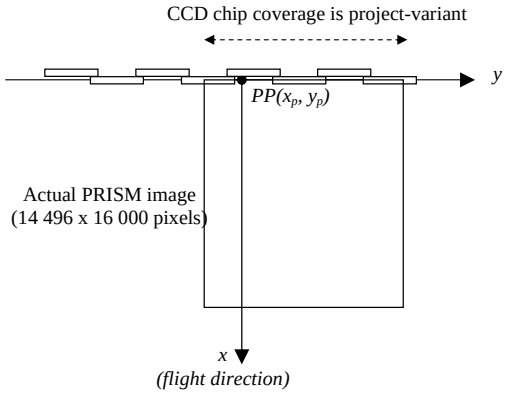

Figure 3. The backward and forward imaging lines contain 8 CCD chips. 32 pixels are located in the overlapping area. There is one coordinate system definition per camera (*x*: flight direction; *y*: CCD line direction). The camera's principal point is the origin of the image coordinate system.

The self-calibration method applies corrections to the image measurements (x_{ij} , y_{ij}) of each point *i* in image *j*. The right hand side of the collinearity equations are extended by correction terms Δx_{ij} and Δy_{ij}:

$$x_{ij} = -c_j \frac{f_x}{f_z} + \Delta x_{ij}$$

$$y_{ij} = -c_j \frac{f_y}{f_z} + \Delta y_{ij}$$

The terms Δx_{ij} and Δy_{ij} include the additional parameters (APs) used to model the systematic errors. The APs are defined separately for each PRISM camera (forward, nadir and backward). The AP set of each image includes:

– 1 scale effect in *y* direction (per image),
– 1 CCD line bending parameter (per image),
– 2 x 4 = 8 displacements of the centres of the CCD chips from the principal point (per image).

The mathematical expressions of the correction terms Δx_{ij} and Δy_{ij} are:

$\Delta x_{ij} = \Delta x_{nj} + y_{ij} r_{ij}^2 b_j$
$\Delta y_{ij} = \Delta y_{nj} + y_{ij} s_j$

with

i = 1,…, m; m = number of points
j = 1,…, 3 number of cameras
n = 1,..., 4 number of CCD chips per focal plane
x_{ij} , y_{ij} : image coordinates of each point *i* in image (camera) *j*
Δx_{nj}, Δy_{nj}: displacement of the centre of each CCD chip *n* from the principal point of the relevant camera *j*
b_j : CCD line bending parameter for the CCD line in each camera *j*
s_j : scale parameter for each camera *j*
$r_{ij}^2 = x_{ij}^2 + y_{ij}^2$

The AP definition and testing have been performed in two different phases of the project. During the first phase, laboratory calibration data for the CCD chip positions and the camera focal lengths were not available. We have observed systematic errors in image space, which indicated displacements in the relative positions of the CCD chips, in all three images (see also Gruen et al., 2007, Kocaman and Gruen, 2007). However, these shifts could be compensated by self-calibration parameters.

In the second phase of the AP tests, we received laboratory calibration data for the PRISM cameras from JAXA, which proved our findings of the self-calibration. Using the laboratory calibration data as input to the adjustment, the AP significance pattern changed. The relative displacements of the CCD chip centers are not significant anymore in our current test results. The significances of the CCD line bending and the scale parameters vary with the project.

3. EMPIRICAL TESTS

We have so far processed data over 4 testfields: Piemont, Italy, Saitama, Japan, Bern/Thun, Switzerland, and Okazaki, Japan. The DGR model and the PPM are used for the orientation tests. Up to two segments per image trajectory have been defined for the PPM. The self-calibration is applied in all tests. The significances of the CCD bending parameters and the scale parameters vary with the dataset. All test results presented in the following sub-sections are obtained with self-calibration for both trajectory models.

The Saitama, Okazaki, and the Bern/Thun datasets are tested with 5, 9 and 25 GCPs to observe the effect of the number of GCPs on the accuracy. The Piemont results are computed only with 5 and 9 GCPs, due to the availability of only a smaller number of GCPs.

The a priori stochastic models of the DGR model and the PPM are the same for all three datasets. The a priori standard deviations of the trajectory position values are 2 m in all 3 directions. Since the trajectory attitude values were not provided for all datasets, they are estimated in the adjustment using low constraints. The accuracies of the GCPs are considered as 0.5 m in planimetry and height. The a priori standard deviation of the image measurements is considered as half a pixel. For the accuracy assessment, the RMSE values, which are computed from the differences of the given and the estimated coordinates of the check points, and the standard deviations, computed from the covariance matrix of unknowns, are used.

After the initial Saitama tests with 30 APs and using the laboratory calibration data, the CCD chip positions are found insignificant. The empirical tests given in the following sections employ self-calibration with 2 APs per image (6 APs in total).

3.1 Saitama Testfield, Japan

The Saitama testfield is located in the north-east of Tokyo, Japan. The testfield has been prepared by JAXA as the first PRISM Cal/Val dataset. The PRISM images have been acquired in April, 2006. The main parameters of the dataset are given in Table 1. There are 203 ground control points measured on the images. The image measurements of the GCPs have been performed by JAXA. Extra tie points were measured at our Institute, due to uneven distribution of the GCPs.

Table 1. Main parameters of the PRISM dataset acquired over the Saitama testfield.

Imaging Date	30.04.2006
Number of PRISM images	1 image triplet
Viewing angles	-23.8°, 0°, 23.8°
Total number of GCPs	203
No. of tie points	111

The dataset is tested using the DGR and the PPM with two segments per trajectory. A brief overview of the accuracy results is given in Table 2. A graphic representation of the RMSE and standard deviation values (std.dev.), which were computed for the ground coordinates of the check points, are given in Figure 4. The check points are a subset of the GCPs, which are not used as control points in the adjustment. The sigma naught of all 6 tests vary between 0.36-0.40 pixels.

Table 2. The DGR and the PPM results of Saitama tests with self-calibration and with 5, 9 and 25 GCP configurations. The results are in meters.

GCP no.	*5*	*5*	*9*	*9*	*25*	*25*
Model	*DGR*	*PPM-2*	*DGR*	*PPM-2*	*DGR*	*PPM-2*
$RMSE_{XY}$	1.38	2.10	1.24	1.25	1.24	1.34
Max_{XY} *Residual*	2.83	4.04	2.62	2.52	2.47	2.91
$RMSE_Z$	2.46	2.77	2.13	2.33	2.00	2.30
Max_Z *Residual*	5.86	6.49	5.77	5.87	5.36	5.58
σ_{XY}	0.79	1.52	0.74	0.86	0.71	0.70
Max σ_{XY}	0.91	2.27	0.83	1.04	0.77	0.78
σ_Z	2.10	2.76	1.98	2.18	1.92	1.89
Max σ_Z	2.43	3.57	2.26	2.46	2.13	2.14
σ_0 *	0.38	0.36	0.38	0.36	0.40	0.37

** Sigma naught is given in pixel*

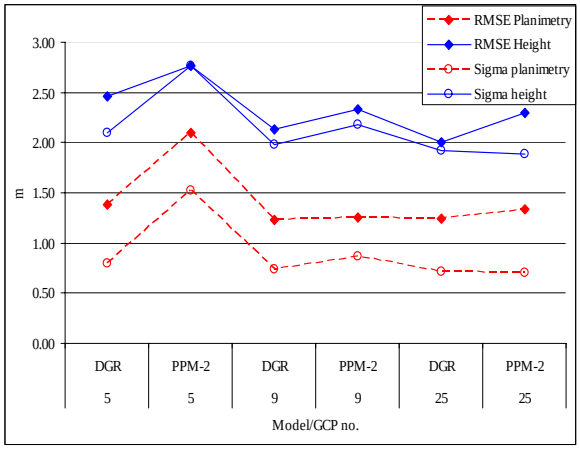

Figure 4. Saitama tests accuracy results (RMSEs and standard deviations, computed for check point coordinates).

With the DGR and the PPM, the RMSE values in planimetry are well at sub-pixel level, even with only 5 GCPs. For DGR, there is not much to gain by going from 5 over 9 to 25 GCPs. The RMSE values in height are similar in all tests. When the DGR and the PPM models are compared, the accuracy values are about at the same level in the 9 and 25 GCPs versions. The PPM requires a higher number of control points to be stable. The instability of the PPM is indicated by the theoretical values (sigma) of the 5 GCPs case, which show significant differences between both models, although the sigma naught is almost equal. In all cases the standard deviations are better than the related RMSEs. This points towards the existence of small systematic residual errors.

3.2 Bern/Thun Testfield, Switzerland

The Bern/Thun testfield has been established by the IGP, ETH Zurich. The testfield in its current form with 108 GCPs and three sub-areas of height reference data was set up under a contract with JAXA. The coordinates of the GCPs were determined by GPS. The project parameters of the PRISM dataset in this testfield are given in Table 3. 82 of the GCPs could be measured in the PRISM images.

Table 3. Main parameters of the PRISM dataset acquired over the Bern/Thun testfield

Imaging Date	21.09.2006
Number of PRISM images	1 image triplet
Viewing angles	-23.8°, 0°, 23.8°
Total number of GCPs	82
No. of tie points	24

The DGR and the PPM with two segments per trajectory are tested separately for comparison. The results of triangulation are given in Table 4. The accuracy both in planimetry and height, as evidenced by $RMSE_{XY}$ and $RMSE_Z$, is below one pixel in all DGR tests. The PPM is instable with a small number (5) of GCPs. A graphical representation of the RMSEs and standard deviations computed from all check points is given in Figure 5. The a posteriori sigma naught values range between 0.37-0.53 pixels. It is somewhat surprising that in some cases the height standard deviations are larger than the related RMSEs.

Table 4. The DGR model and the PPM results with self-calibration and with 5, 9 and 25 GCP configurations. The results are in meters

GCP no.	*5*	*5*	*9*	*9*	*25*	*25*
Model	*DGR*	*PPM-2*	*DGR*	*PPM-2*	*DGR*	*PPM-2*
$RMSE_{XY}$	2.23	4.35	1.97	3.47	1.80	1.93
Max_{XY} *Residual*	4.59	10.75	4.37	6.30	3.47	3.45
$RMSE_Z$	1.77	5.24	1.57	3.30	1.46	3.21
Max_Z *Residual*	4.80	12.82	4.63	8.40	4.45	8.45
σ_{XY}	0.82	2.52	0.75	0.99	0.89	1.01
Max σ_{XY}	1.10	4.44	1.04	1.34	1.19	1.30
σ_Z	2.09	6.51	2.01	2.62	2.43	2.77
Max σ_Z	3.60	13.14	3.54	4.80	4.21	4.58
σ_0 *	0.37	0.38	0.37	0.39	0.50	0.53

* *Sigma naught is given in pixel*

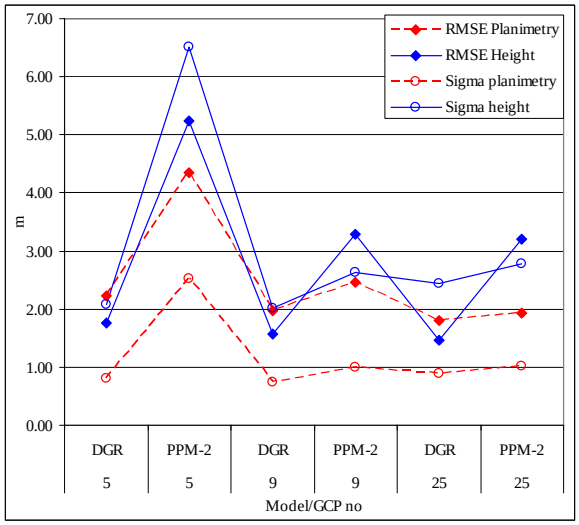

Figure 5. Bern/Thun tests accuracy results (RMSEs and standard deviations, computed for check point coordinates).

3.3 Piemont Testfield, Italy

The Piemont testfield is located in the north-western part of Italy. The testfield was set up by GAEL, France. The coordinates of the GCPs were determined by GPS. The main parameters of the PRISM dataset are given in Table 5.

Table 5. Main parameters of the PRISM dataset acquired over the Piemont testfield

Imaging Date	04.09.2006
Number of PRISM images	1 image triplet
Viewing angles	-23.8°, 0°, 23.8°
Total no. of GCPs	29
Total no. of tie points	142

The DGR model and the PPM have been tested with two different GCP configurations and the results are given in Table 6. The graphical representation of the results is shown in Figure 6. The accuracy values are at sub-pixel level for all models. The DGR model performs again better than the PPM in the 5 GCPs configuration. The a posteriori sigma naught values are very similar in all tests and vary between 0.27-0.29 pixels.

Also here it is somewhat surprising that all height standard deviations are bigger than the related RMSEs.

Table 6. The DGR model and the PPM results with self-calibration and with 5 and 9 GCP configurations. The results are in meters.

GCP no.	*5*	*5*	*9*	*9*
Model	*DGR*	*PPM-2*	*DGR*	*PPM-2*
$RMSE_{XY}$	2.34	2.58	2.22	2.20
Max_{XY} *Residual*	3.71	4.10	3.55	4.19
$RMSE_Z$	1.05	2.36	1.03	1.20
Max_Z *Residual*	2.36	4.84	2.04	2.18
σ_{XY}	0.58	2.37	0.59	0.68
Max σ_{XY}	0.67	6.66	0.70	1.40
σ_Z	1.60	4.10	1.64	1.82
Max σ_Z	1.84	10.68	1.94	3.23
σ_0 *	0.27	0.25	0.29	0.26

** Sigma naught is given in pixel*

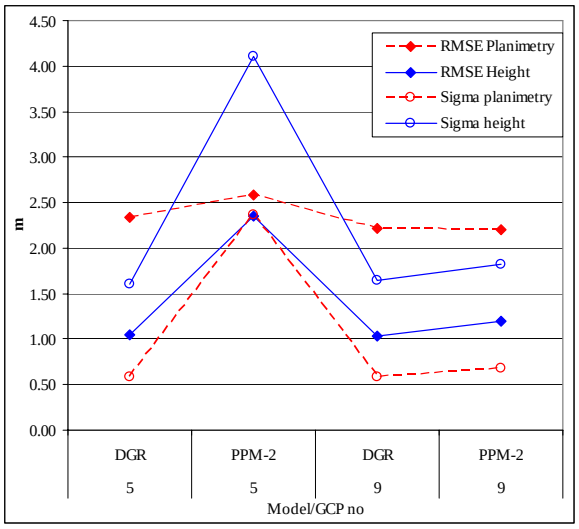

Figure 6. Piemont tests accuracy results (RMSEs and standard deviations, computed for check point coordinates).

3.4 Okazaki Testfield, Japan

The Okazaki testfield is located in the Aichi Prefecture on the Honshu island of Japan. The testfield has been generated as the 2nd ALOS/PRISM Cal/Val dataset by JAXA. The main project parameters are given in Table 7. The DGR results with 5, 9, and 25 GCP configurations and the PPM results with 25 GCPs are presented in Table 8. A graphic representation of the RMSE and standard deviation values, which were computed for the ground coordinates of the check points, are given in Figure 7. Since the Okazaki tests were performed after all other testfields, the PPM is not applied with a small number of GCPs. Only the 25 GCPs configuration is used and the whole trajectory is modelled with one segment only.

Using the DGR model, there is not much to gain from 5 to 25 GCPs in planimetric accuracy. However, the height accuracy improves with the increase of the number of GCPs. The a posteriori sigma naught values are very similar in all tests and vary between 0.51-0.54 pixels.

Table 7. Main parameters of the PRISM dataset acquired over the Okazaki testfield.

Imaging Date	20.06.2006
Number of PRISM images	1 image triplet
Viewing angles	-23.8°, 0°, 23.8°
Total number of GCPs	51
No. of tie points	135

Table 8. Okazaki testfield, the DGR model and the PPM results with self-calibration and with 5 and 9 GCP configurations. The results are in meters.

GCP no.	*5*	*9*	*25*	*25*
Model	*DGR*	*DGR*	*DGR*	*PPM-1*
$RMSE_{XY}$	1.98	1.92	1.92	1.97
Max_{XY} *Residual*	4.86	5.06	4.96	4.88
$RMSE_Z$	3.13	2.41	1.85	1.80
Max_Z *Residual*	7.01	5.47	4.44	4.54
σ_{XY}	1.12	0.97	0.94	0.93
Max σ_{XY}	1.28	1.06	0.97	0.98
σ_Z	2.95	2.62	2.56	2.54
Max σ_Z	3.36	2.87	2.64	2.62
σ_0 *	0.51	0.51	0.54	0.53

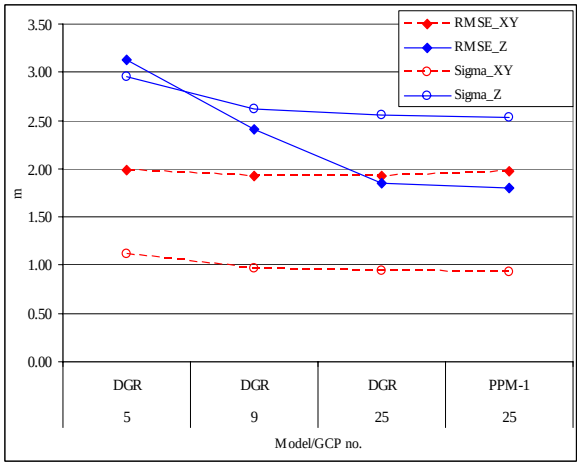

Figure 7. Okazaki tests accuracy results (RMSEs and standard deviations, computed for check point coordinates)

4. CONCLUSIONS

We have calibrated and validated early ALOS/PRISM images over four testfields: Piemont, Italy, Saitama, Japan, Bern/Thun, Switzerland, and Okazaki, Japan. We calibrated the PRISM system using the technique of self-calibration. In all cases we used PRISM image triplets. Validation is a system approach. It includes the sensor performance, but also the quality of both the data processing algorithms and the reference data. The validations of our georeferencing procedures could be performed in all 4 testfields.

We started our calibration approach with partially uncalibrated Saitama image data. The missing information concerning the precise location of the individual focal plane array CCD chips with respect to the camera's principal point led to significant systematic errors in object and image space. By applying the respective additional parameters in our self-calibration procedure (2 shifts for each chip in image space) we were able

to compensate these systematic errors, thus leading to much better results (improvement of up to 50%).

After receiving from JAXA the calibrated shift values for the chips we applied those and found the results correct after validation by self-calibration.

For georeferencing we applied both our sensor/trajectory models DGR and PPM and found that DGR had the better performance in case of very few GCPs. Under the given sensor configurations the PPM method turned out to be a bit instable with 5 GCPs, but with 9 and more GCPs both methods performed equally well overall.

If we only consider the DGR results here we achieved over all 4 testfields the following average values:
+ Planimetric accuracy RMSE(X,Y) = 1.2 - 2.3 m
  Sigma (X,Y) = 0.58 - 0.94 m
+ Height accuracy RMSE(Z) = 1.0 - 2.5 m
  Sigma (Z) = 1.6 – 2.6 m
+ Estimated accuracy of image coordinates Sigma0 =
  0.27 – 0.54 pixel

We note that in some cases the empirical height accuracy values (RMSE(Z)) are even better than the corresponding theoretical precision values.

Over all 4 testfields we achieved with our empirical accuracy values quite consistent results: We stay in all cases in the sub-pixel domain, in the best cases we achieved about half a pixel accuracy. This relatively high accuracy is surprising considering the fact that the image quality of PRISM has much potential for improvement.

By analysing the check point residuals we note that there are still small systematic errors left in the results. This is a topic for further investigations.

Self-calibration is a very powerful method for sensor model refinement. However, the most appropriate additional parameter functions have not yet been fully explored for PRISM imagery. In any case, self-calibration should be used with great care and not blindly. The statistical testing of additional parameters for determinability is a crucial requirement for a successful use of this technique.

If we compare these georeferencing and matching results with those which were obtained with other satellite sensors of similar type (SPOT-5, IKONOS) we note that the accuracy (expressed in pixels) is about the same as with IKONOS, but less good than SPOT-5.

This is fully in line with our expectations and can be attributed to the differences in image configuration (PRISM was used in triplet mode, the others in stereo mode) on the one side and to the inferior image quality of PRISM on the other side.

REFERENCES

Baltsavias E. P., Pateraki M., Zhang L., 2001. Radiometric and Geometric Evaluation of IKONOS Geo Images and Their Use for 3D Building Modeling. In Proceedings of Joint ISPRS Workshop on "High Resolution Mapping from Space 2001", 19-21 September, Hannover, Germany (on CD-ROM).

Eisenbeiss H., Baltsavias E. P., Pateraki M., Zhang L., 2004. Potential of IKONOS and QUICKBIRD Imagery for Accurate 3D-Point Positioning, Orthoimage and DSM Generation. International Archives of Photogrammetry, Remote Sensing and Spatial Information Sciences, 35 (B3), pp. 522-528.

Fraser C., Baltsavias E. P., Gruen A., 2002. Processing of IKONOS Imagery for Sub-meter 3D Positioning and Building Extraction. ISPRS Journal of Photogrammetry & Remote Sensing, 56(3), pp. 177-194.

Fraser C., Hanley H. B., 2003. Bias Compensation in Rational Functions for IKONOS Satellite Imagery. Photogrammetric Engineering and Remote Sensing, 69(1), pp. 53-57.

Grodecki J., Dial G., 2003. Block Adjustment of High-Resolution Satellite Images Described by Rational Polynomials. Photogrammetric Engineering and Remote Sensing, 69(1), pp. 59-68.

Gruen A., Beyer H.A., 2001. System Calibration Through Self-Calibration. Calibration and Sensor Orientation of Cameras. In Computer Vision, Eds. Gruen, Huang, Springer-Verlag Berlin, Heidelberg, pp.163-193.

Gruen A., Zhang L., 2003. Sensor Modeling for Aerial Triangulation with Three-Line-Scanner (TLS) Imagery. Journal of Photogrammetrie, Fernerkundung, Geoinformation (PFG), 2/2003, pp. 85-98.

Gruen A., Zhang L., Eisenbeiss H., 2005. 3D Precision Processing Of High Resolution Satellite Imagery. ASPRS 2005, Baltimore, Maryland, USA, March 7-11 (on CD-ROM).

Gruen A., Kocaman S., Wolff K., 2007. Calibration and Validation of Early ALOS/PRISM Images. The Journal of the Japan Society of Photogrammetry and Remote Sensing, Vol 46, No. 1, pp. 24-38.

Iwata T., 2003. Precision Geolocation Determination and Pointing Management for the Advanced Land Observing Satellite (ALOS). IEEE/IGARSS 2003, Toulouse, France, July 21-25.

Jacobsen K., 2003. Geometric Potential of IKONOS and QuickBird-Images. Photogrammetric Week ’03, Ed. D. Fritsch, pp. 101-110.

Kocaman S., 2003. Self-calibrating Triangulation with TLS Imagery. Internal Technical Report, ETH Zurich, Institute of Geodesy and Photogrammetry, 26 June.

Kocaman S., Zhang L., Gruen A., 2006. Self-calibrating Triangulation of Airborne Linear Array CCD Cameras. EuroCOW 2006 International Calibration and Orientation Workshop, Castelldefels, Spain, 25-27 Jan. (on CD-ROM).

Kocaman S., Gruen A., 2007. Orientation and Calibration of ALOS/PRISM Imagery, High-Resolution Earth Imaging for Geospatial Information, Proceedings of ISPRS Hannover Workshop 2007, Hanover, Germany.

Poli D., 2005. Modelling of Spaceborne Linear Array Sensors. Ph. D. Dissertation, IGP Report No. 85, ISSN 0252-9335 ISBN 3-906467-3, Institute of Geodesy and Photogrammetry, ETH Zurich, Switzerland.

Tadono T., Shimada M., Watanabe M., Hashimoto T., Iwata T., 2004. Calibration and Validation of PRISM Onboard ALOS. International Archives of Photogrammetry, Remote Sensing and Spatial Information Sciences, Vol.XXXV part B1, pp. 13-18.